ELSEVIER

FEBS Letters 337 (1994) 88–92

FEBS 13497

FEBS LETTERS

Structure of partially-activated *E. coli* heat-labile enterotoxin (LT) at 2.6 Å resolution

Ethan A. Merritt[a], Sylvia E. Pronk[b], Titia K. Sixma[b,**], Kor H. Kalk[b], Ben A.M. van Zanten[b], Wim G.J. Hol[a,*]

[a]*Department of Biological Structure SM-20, University of Washington, Seattle, WA 98195, USA*
[b]*Bioson Research Institute, University of Groningen, Nijenborgh 4, 9747 AG Groningen, The Netherlands*

Received 15 November 1993

Abstract

Biological toxicity of *E. coli* heat-labile enterotoxin and the closely related cholera toxin requires that the assembled toxin be activated by proteolytic cleavage of the A subunit and reduction of a disulfide bond internal to the A subunit. The structural role served by this reduction and cleavage is not known, however. We have crystallographically determined the structure of the *E. coli* heat-labile enterotoxin AB_5 hexamer in which the A subunit has been cleaved by trypsin between residues 192 and 195. The toxin is thus partially activated, in that it has been cleaved but the disulfide bond has not been reduced. The structure of the A subunit in the cleaved toxin is substantially the same as that previously observed for the uncleaved AB_5 structure, suggesting that although such cleavage is required for biological activity of the toxin it does not by itself cause a conformational change.

Key words: Heat-labile enterotoxin; Cholera toxin; ADP-ribosylation

1. Introduction

The heat-labile enterotoxin (LT) from *E. coli* is a member of a class of medically important bacterial toxins which act intracellularly to catalyze ADP-ribosylation of specific cell proteins. These toxins share an A/B functional organization in which the B fragment mediates specific binding to cell surface receptors while the A fragment contains the enzymatic activity. In the case of LT and the 80% sequence-identical cholera toxin (CT), the holotoxin forms an AB_5 hexamer. In both LT and CT a pentamer of identical B subunits binds specifically to the terminal oligosaccharide of ganglioside G_{M1} protruding from the intestinal epithelial cell membrane. In both toxins toxicity is due to catalytic activity of the A subunit in the cytosol of the target cell, where it causes ADP-ribosylation of the α subunit of the G_s regulatory protein. Both LT and CT cause diarrheal disease and dehydration, although the severity of the disease caused by enterotoxigenic *E. coli* is much less than that of cholera.

We have previously reported the structure of the LT AB_5 holotoxin at 1.95 Å resolution [1,2]. The LT A subunit consists in the holotoxin of a single peptide chain containing 240 residues [3,4]. Its tertiary structure clearly consists of two domains (Fig. 1). The bulk of the subunit comprises the roughly conical A_1 domain containing an irregular α/β secondary structure. The smaller A_2 domain consists of a 23-residue α-helix near the carboxy-terminal extending from the A_1 domain to the flat base of the B_5 pentamer and terminating in an extended chain which spans the central pore of the B_5 pentamer and serves to link the A subunit to the B pentamer. Catalytic activity is located solely on the A_1 fragment [5]. For full activity the two domains must be separated by proteolytic cleavage of the main chain and also by reduction of the disulfide bond ($CysA^{187}$– $CysA^{199}$) linking A_1 and A_2 [6–8]. The short peptide chain linking the two domains (approximately residues 183–196) is only partially visible in the X-ray structure of the intact holotoxin, and is presumed to be a flexible loop containing the proteolytic cleavage site. In *V. cholerae* an endoprotease is present which nicks the A subunit of CT to separate A_1 and A_2 [9]. In *E. coli* no such protease is present and the LT toxin is instead activated later by a protease in the host cell which cleaves somewhere between residues 192 and 195. It is not entirely clear why the cleavage and reduction are required. Possible explanations include direct linkage of disulfide reduction with membrane translocation, a hypothetical requirement for the A_1 fragment to be separated from the rest of the toxin for efficient membrane translocation, exposure or increased

*Corresponding author. Fax: (1) (206) 543 1524.

***Present address:* Department of Molecular Biophysics and Biochemistry, Yale University, BCMM 154, 295 Congress Avenue, New Haven, CT 06510, USA.

SSDI 0014-5793(93)E1414-H

Fig. 1. Three-dimensional representation of LT AB_5 structure (program MOLSCRIPT [22]). The two domains of the A subunit are clearly visible, with A_1 forming an inverted cone at the upper left of the figure, and A_2 comprising the long helical region whose tail extends through the central pore of the B pentamer. Sidechains of residues implicated as active site residues are shown in ball and stick representation, as is the disulfide bridge between residues A187 and A199. The cleavage site is located at the juncture of the two domains, and is physically remote from the region of the A_1 domain tentatively identified as the active site. For clarity, the B subunits are depicted as a simplified backbone tracing so that the carboxy-terminus of the A subunit (RDEL signal sequence) is not obscured.

accessibility of the substrate binding site, or a possible conformational change which promotes catalysis. The present report describes the crystallographically determined structure at 2.6 Å resolution of the LT AB_5 holotoxin in which the peptide chain of the A subunit has been cleaved, but the linking disulfide bond has not been reduced.

2. Experimental

Purified heat-labile enterotoxin from porcine *E. coli* [10] was concentrated in TEA buffer (100 mM Tris, 1 mM EDTA, 0.02% sodium azide) and 0.2 M NaCl to a protein concentration of 17 mg/ml. Proteolysis was conducted by incubating 125 μl of the protein solution at room temperature with 5 μl of trypsin at a concentration of 5 mg/ml. After 30 min proteolysis was stopped by addition of 5 μl of BPTI at a concentration of 3 mg/ml. To confirm that the A chain of the toxin had in fact been cleaved, the treated protein was run on SDS-PAGE in the presence of β-mercaptoethanol (Fig. 2). Crystallization was carried out using a variant of the three-layer liquid–liquid diffusion procedure described in [10]. Crystallographic data collection is summarized in Table 1.

A starting crystallographic model for the protein chains was taken from the refined 1.95 Å structure of the native LT AB_5 [2]. An initial round of refinement in which the five copies of the B subunit were treated as rigid bodies, and four regions of the A subunit chain were similarly treated, brought the crystallographic R factor to $R = 0.26$. Subsequent refinement of individual positional and isotropic thermal parameters for the protein atoms produced a value of $R = 0.20$. At this point the fit of the model protein chain to the observed electron density was evaluated and optimized in a series of $(F_o–F_c)$ electron density maps covering the entire toxin molecule. In each map approximately 50 residues (~7% of the total structure) were omitted from the calculation of F_c. A model for the discretely ordered solvent was constructed incrementally by identifying peaks from successive $(F_o–F_c)$ maps. Before each incremental map calculation all proteins atoms and previously identified solvent sites were refined. The final solvent model contains 197 discretely ordered waters, each of which exhibited electron density at greater than 3σ and acceptable hydrogen-bonding geometry. Continued refinement achieved a final crystallographic R value of 0.172 for a model including a small overall anisotropic B correction (Table 1). All crystallographic refinement was carried out using X-PLOR version 2.1 [11].

3. Results

Electron density for residues 189–195 of the A subunit, within which the proteolytic cleavage site lies, was not visible in the original LT X-ray structure at 1.95 Å resolution nor is it visible in the present structure of the cleaved toxin. This is consistent with the cleavage site lying on a flexible loop accessible to protease, but unfortunately does not permit us to inspect the actual cleavage site in the crystallographic model. Nevertheless, one might expect the cleavage to allow or induce conformational changes or additional flexibility in neighboring regions of the structure. Such changes are not seen, however, in the present structure. The overall RMS difference in main-chain coordinates observed for the A subunit between the 1.95 Å holotoxin structure and the present structure is only 0.21 Å (Fig. 3A), compared with an

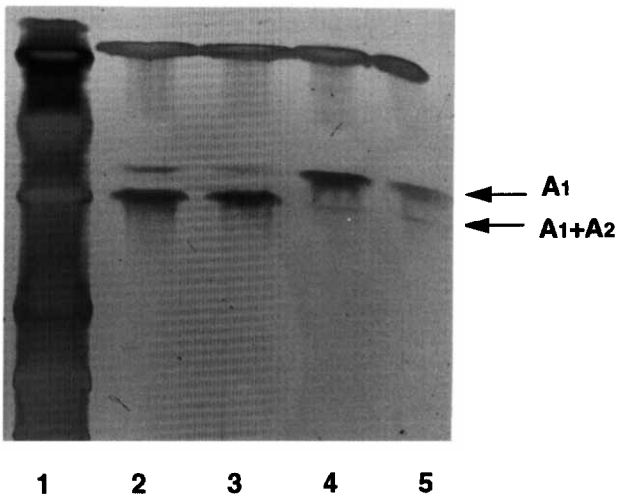

Fig. 2. SDS-polyacrylamide gel electrophoresis of LT prior to crystallization. Lane 1, markers; lane 2, LT prior to trypsin cleavage; lane 3, LT + dithiothreitol; lane 4, LT after trypsin cleavage (crystallization condition); lane 5, LT after trypsin cleavage + dithiothreitol. Note that the gel is run in the presence of β-mercaptoethanol, so that the disulfide bond linking A_1 and A_2 is reduced in all cases; i.e. the presence or absence of prior treatment with dithiothreitol is not distinguishable on this gel.

overall RMS difference of 0.27 Å for all atoms in the six protein subunits. Although the largest difference is observed as expected for the residues immediately adjacent to the flexible loop (188A, 196A–198A), this shift does not propagate to residues which are nearby either spatially or sequentially. The largest remaining differences between the two sets of coordinates for the A subunit are seen in the regions A32–A37 and A75–A80. Since these are also the residues with the highest thermal parameters in both structures, the larger difference in refined coordinates is most likely due purely to intrinsic uncertainty in the models due to thermal motion in these regions. The orientation of the A_1 or A_2 fragments relative to each other or to the B pentamer differs by less than 0.25° from what is seen in the uncleaved structure.

The average thermal parameter B for all protein atoms in the present 2.6 Å model of the cleaved structure is 19.3 Å^2 (B_{avg} = 23.7 Å^2 for the A subunit, B_{avg} = 17.4 Å^2 for the B pentamer). This is somewhat lower than that found for the 1.95 Å model for the uncleaved structure (Fig. 3B), but is consistent with other LT data sets we have refined ([2,12], also unpublished results). It may nevertheless be worth noting that the B values for the main-chain atoms immediately adjacent to the cleavage site are relatively lower in the present cleaved structure than they were in the original uncleaved structure.

Table 1
Crystallographic data for partially activated LT

Data used in refinement:	21320 reflections 10 Å–2.6 Å, no cut-off on $I/\sigma(I)$
Model:	6175 atoms contributing to F_c 197 water molecules in solvent model
Crystallographic R:	0.173 with no overall B correction 0.172 with overall anisotropic B correction: B_{11} = 0.01573 B_{22} = −0.03028 B_{33} = 0.02301 B_{12} = 0.00763 B_{13} = 0.01256 B_{23} = −0.00713
Stereochemistry:	0.015 Å RMS deviation from ideal bond lengths 3.24° RMS deviation from ideal bond angles

Crystallization of the trypsin-nicked enterotoxin was performed using liquid–liquid diffusion in glass capillaries. Successive layers consisting of 5 μl of protein solution after proteolysis as described above, 10 μl of 50 mM fructose in TEA, and 5 μl of 6% PEG 6000 in TEA were applied on top of each other in glass capillaries. The middle layer contained a non-binding sugar (fructose) to slow down nucleation of the crystals. During two weeks of storage at room temperature crystals formed in space group $P2_12_12_1$ with cell dimensions essentially identical to crystals of the uncleaved AB_5 holotoxin (a = 119.2 Å, b = 98.2 Å, c = 64.8 Å, one AB_5 hexamer per a.s.u.). Crystallographic data were measured from a single crystal at room temperature using an Enraf-Nonius FAST area detector mounted on an Elliot G21 rotating anode. 47,662 observations from ∞ to 2.6 Å were processed with programs MADNES [23] and XDS [24] to give 21,707 unique reflections to 2.6 Å (90% complete, R_{sym} = 0.086).

4. Discussion

Many bacterial protein toxins are produced in a proenzyme form, and must be activated by subsequent processing during secretion or during entry into the target cell. For LT and CT both proteolysis of the A subunit and reduction of the 187–199 disulfide bond are required for activation [6,7]. In determining the mechanistic significance of these activation steps it may be instructive to consider what is known of the activation process for other related toxins. Shiga toxin and shiga-like toxins are structurally similar to LT and CT in that they assemble as AB_5 assemblages, and their A subunits can be split into A_1 and A_2 fragments of similar sizes by cleavage in a protease labile region. In vitro activation of shiga toxin requires nicking in the presence of DTT and SDS [13,14]. The enzymatic activity of the shiga toxins is different from that of LT and CT, however, and there is no significant sequence homology. *Pseudomonas* exotoxin and diphtheria toxin, on the other hand, catalyze the same ADP-ribosylating reaction as LT and have considerable functional similarity in the enzymatic domain, but have a very different subunit structure [1,15,16]. Both exotoxin and diphtheria toxin are activated by cleavage and reduction of a disulfide loop, and the details are somewhat better known than for the equivalent activation of LT. The catalytic C domain of diphtheria toxin is connected to the remainder of the protein by a flexible loop anchored at the base by an inter-domain disulfide bridge between residues 186 and 200 [16]. This loop must be cleaved for activation, but the precise nature of the cleavage site is unimportant [17]. For diphtheria toxin reduction of the disulfide bond is the rate-limiting step in intoxication, and occurs prior to or coincident with translocation from an endosomal compartment to the cytoplasm [18,19]. Exotoxin A is cleaved between Arg^{279} and Gly^{280} by an intracellular protease [15], and is similarly reduced in an endosomal compartment prior to or coincident with translocation [20].

Thus there are a number of bacterial toxins which require a proteolytic cleavage of a flexible region irrespective of enzymatic activity or subunit structure, and certainly without identifiable sequence homology. Even between LT and CT there are 6 sequence differences in the loop from 183–196 [4], substantially less homology than is present between the sequences as a whole. Thus a flexible region needed for toxin activation is a conserved feature but the actual cleavage site is not very important. In the course of evolution many rearrangements of subunit structures have occurred in these multisubunit toxins. Why then do these toxins conserve such a proteolytic site rather than splitting into separate subunits? A plausible model is that the A_2 fragment holds structural features necessary for internalization of the toxin or proper targeting to the cellular compartment where the toxin acts. A close association of A_1 and A_2

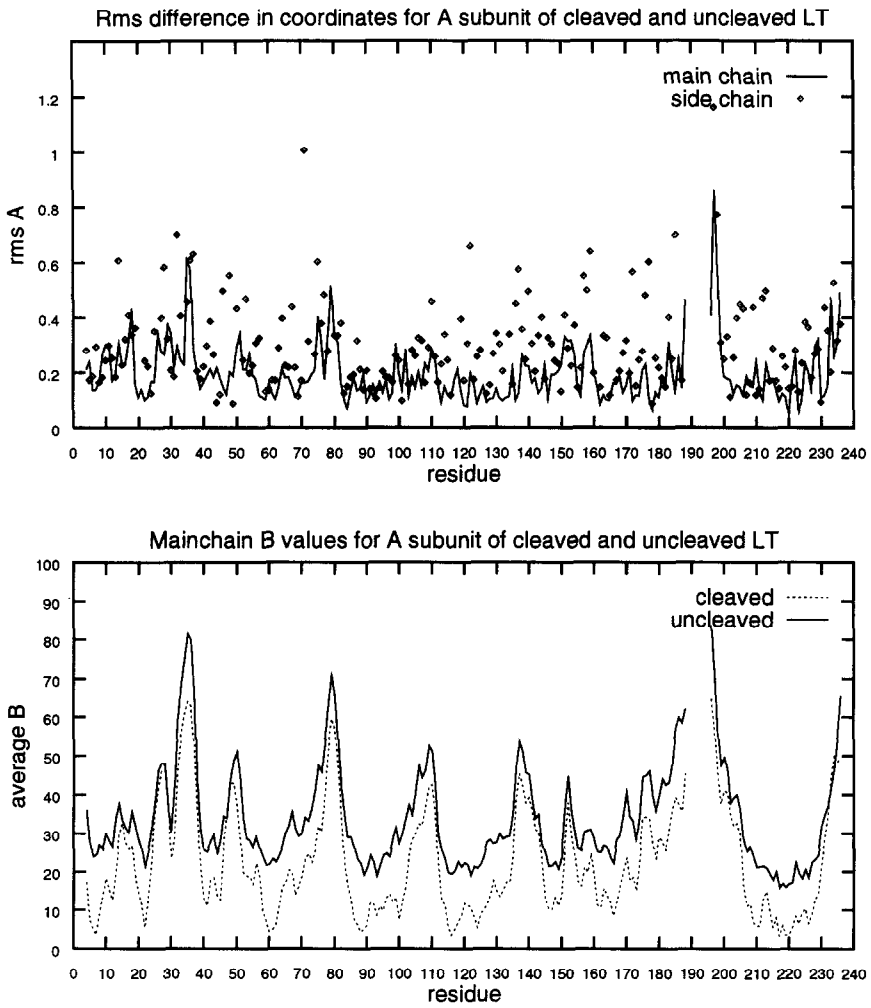

Fig. 3. (A) RMS difference in coordinates (Å) for the A subunit between the crystallographic models for the cleaved (present communication) and uncleaved [2] structures. Solid line = main-chain atoms; individual points = sidechain atoms. (B) Average thermal parameters B (Å^2) for mainchain atoms in the A subunit of the LT AB_5 holotoxin in the cleaved (present communication) and uncleaved [2] forms.

is then required to bring the enzymatically active A_1 to its site of action. Following the model of diphtheria toxin, the reduction of the disulfide (or, more speculatively, a recognition event involving the dangling ends of the flexible region subsequent to cleavage) is coincident with the final stage(s) of the intracellular transport process, after which the presence of the A_2 fragment is superfluous. In this context it is also notable that the C-terminal sequence of the A_2 domain in LT is RDEL, known to be a signal sequence in eukaryotic cells which causes targeting of the protein to the endoplasmic reticulum (review, see [21]). How this signal sequence might function in targeting a protein entering the cell from the outside remains to be explored. Finally, Moss et al. [8] have shown that both reduction and cleavage are required for the toxin to bind the ADP-ribosylation factor (ARF) protein. While the location of the ARF binding site on the toxin is not known, this result suggests that it may lie on the surface of the A_1 fragment which is obscured by the presence of A_2 prior to reduction and cleavage.

The lack of any substantial conformational difference between the cleaved and uncleaved structures implies that cleavage of the peptide chain does not play a primary role in the biological activation of the toxin. Since the disulfide bond between residues A187 and A199 closely brackets the cleavage site it is likely that even after cleavage the peptide chains are held in their original conformation by the disulfide bridge. Only upon reduction of this disulfide would a conformational change in the A_1 fragment, if any, take place. We are presently exploring the feasibility of further structural studies of the toxin after reduction.

Acknowledgements: We gratefully thank Mr. Jaap Kingma and Dr. B. Witholt for ample supply of protein material. This work was supported in part by the Dutch Foundation for Clinical Research (SON) with financial aid from the Dutch Organisation for Scientific Research (NWO). Crystallographic coordinates have been deposited with the

Brookhaven Protein Data Bank for immediate release (entry 1LTB).

References

[1] Sixma, T.K., Pronk, S.E., Kalk, K.H., Wartna, E.S., van Zanten, B.A.M., Witholt, B. and Hol, W.G.J. (1991) Nature 351, 371–378.

[2] Sixma, T.K., Kalk, K.H., van Zanten, B.A.M., Dauter, Z., Kingma, J., Witholt, B. and Hol, W.G.J. (1993) J. Mol. Biol. 230, 890–918.

[3] Yamamoto, T., Tamura, T. and Yokota, T. (1984) J. Biol. Chem. 259, 5037–5044.

[4] Yamamoto, T., Gojobori, T. and Yokota, T. (1987) J. Bacteriol. 169, 1352–1357.

[5] Gill, D.M. (1976) Biochemistry 15, 1242–1248.

[6] Mekalanos, J.J., Collier, R.J. and Romig, W.R. (1979) J. Biol. Chem. 254, 5855–5861.

[7] Moss, J., Osborne Jr., J.C., Fishman, P.H., Nakaya, S. and Robertson, D.C. (1981) J. Biol. Chem. 256, 12861–12865.

[8] Moss, J., Stanley, S.J., Vaughan, M. and Tsuji, T. (1993) J. Biol. Chem. 268, 6383–6387.

[9] Xia, Q.-C., Chang, D., Blacher, R. and Lai, C.-Y. (1984) Arch. Biochem. Biophys. 234, 363–370.

[10] Pronk, S.E., Hofstra, H., Groendijk, H., Kingma, J., Swarte, M.B.A., Dorner, F., Drenth, J., Hol, W.G.J. and Witholt, B. (1985) J. Biol. Chem. 260, 13580–13584.

[11] Brünger, A.T. (1990) X-PLOR Version 2.1 Manual, Yale University.

[12] Sixma, T.K., Pronk, S.E., Kalk, K.H., van Zanten, B.A.M., Berghuis, A.M. and Hol, W.G.J. (1992) Nature 355, 561–564.

[13] Reisbig, R., Olsnes, S. and Eiklid, K. (1981) J. Biol. Chem. 256, 8739–8744.

[14] Olsnes, S., Reisbig, R. and Eiklid, K. (1981) J. Biol. Chem. 256, 8732–8738.

[15] Ogata, M., Fryling, C.M., Pastan, I. and FitzGerald, D.J. (1992) J. Biol. Chem. 267, 25396–25401.

[16] Choe, S., Bennett, M.J., Fujii, G., Curmi, P.M.G., Kantardjieff, K.A., Collier, R.J. and Eisenberg, D. (1992) Nature 357, 216–222.

[17] Ariansen, S., Afanasiev, B.N., Moskaug, J.O., Stenmark, H., Madshus, I.H. and Olsnes, S. (1993) Biochemistry 32, 83–90.

[18] Wright, H.T., Marston, A.W. and Goldstein, D.J. (1984) J. Biol. Chem. 259, 1649–1654.

[19] Papini, E., Rappuoli, R., Murgia, M. and Montecucco, C. (1993) J. Biol. Chem. 268, 1567–1574.

[20] FitzGerald, D. and Pastan, I. (1991) Semin. Cell Biol. 2, 31–37.

[21] Pelham, R.B.P. (1991) Curr. Opin. Cell Biol. 3, 585–591.

[22] Kraulis, P. (1991) J. Appl. Crystallogr. 24, 946–950.

[23] Messerschmidt, A. and Pflugrath, J.W. (1987) J. Appl. Crystallogr. 20, 306–315.

[24] Kabsch, W. (1988) J. Appl. Crystallogr. 21, 916–924.